Atmos. Chem. Phys. Discuss., https://doi.org/10.5194/acp-2018-1165
Manuscript under review for journal Atmos. Chem. Phys.
Discussion started: 20 December 2018

Atmospheric Chemistry and Physics
Discussions

Estimation of Hourly Land Surface Heat Fluxes over the Tibetan Plateau by the Combined Use of Geostationary and Polar Orbiting Satellites

Lei Zhong[1], Yaoming Ma[2,3,4], Zeyong Hu[3,5], Yunfei Fu[1], Yuanyuan Hu[1], Xian Wang[1], Meilin Cheng[1], Nan Ge[1]

[1]School of Earth and Space Sciences, University of Science and Technology of China, Hefei 230026, China

[2]Key Laboratory of Tibetan Environment Changes and Land Surface Processes, Institute of Tibetan Plateau Research, the Chinese Academy of Sciences, Beijing 100101, China

[3]CAS Center for Excellence in Tibetan Plateau Earth Sciences, Beijing 100101, China

[4] University of Chinese Academy of Sciences, Beijing 100049, China

[5] Northwest Institute of Eco-Envrionment and Resources, the Chinese Academy of Sciences, Lanzhou 730000, China

Correspondence to: Lei Zhong (zhonglei@ustc.edu.cn)

Abstract. The estimation of land surface heat fluxes has significant meaning for energy and water cycle studies, especially for the Tibetan Plateau (TP), which has unique topography and strong land-atmosphere interactions. The land surface heating status also directly influences the movement of atmospheric circulation. However, for a long time, plateau-scale land surface heat flux information with high temporal resolution has been lacking, which greatly limits understanding of diurnal variations in land-atmosphere interactions. Based on geostationary and polar orbiting satellite data, a surface energy balance system (SEBS) was used in this paper to derive hourly land surface heat fluxes with a spatial resolution of 10 km. Six stations scattered through the TP and equipped for flux tower measurements were used to correct the energy imbalance problem existing in the measurements and to perform cross-validation. The results showed good agreement between derived fluxes and in situ measurements through 3738 validation samples. The RMSEs for net radiation flux, sensible heat flux, latent heat flux and soil heat flux were 76.63 Wm^{-2}, 60.29 Wm^{-2}, 64.65 Wm^{-2} and 37.5 Wm^{-2}, respectively. The derived results were also found to be superior to GLDAS flux products (RMSEs for the surface energy balance components were 114.32 Wm^{-2}, 67.77 Wm^{-2}, 75.6 Wm^{-2} and 40.05 Wm^{-2}, respectively). The diurnal and seasonal cycles of land surface energy balance components were clearly identified. Their spatial distribution was found to be consistent with the heterogeneous land surface status and general hydrometeorological conditions of the TP.

Atmos. Chem. Phys. Discuss., https://doi.org/10.5194/acp-2018-1165
Manuscript under review for journal Atmos. Chem. Phys.
Discussion started: 20 December 2018

1. Introduction

Mass and energy exchanges are constantly carried out between the land surface and the atmosphere above. At the same time, the weather, climate and environmental changes at multiple spatiotemporal scales are greatly influenced by such land-atmosphere exchanges. Land-atmosphere interaction is a popular topic not only in the field of atmospheric research but also in hydrology, geography, ecology and environmental sciences (Ye and Fu 1994). The impacts of land-atmosphere interactions on weather and climate change have been assessed through surface sensible heat flux, latent heat flux and momentum flux (Seneviratne et al, 2008; Ma et al, 2017). How to accurately derive the surface heat fluxes has always been a main research question and a focus of atmospheric science.

The Tibetan Plateau (TP), with an average elevation of more than 4000 m, is also called 'the Third Pole' and 'the World Roof'. The thermal and dynamic effects caused by the TP's high elevation and relief have profound impacts on atmospheric circulation, the Asian monsoon and global climate change (Ye and Gao1979; Ma et al, 2006; Ma et al, 2008; Zhong et al, 2011; Zou et al, 2017; Zou et al, 2018). The interactions between TP multispheres, such as the atmosphere, hydrosphere, lithosphere, biosphere, and cryosphere, are the drivers of all these changes. The TP is also one of the most sensitive regions in response to global climate change (Liu et al, 2000). In recent years, some studies have argued that the major factor impacting the South Asian monsoon is the insulating effect of the southern mountain edges of the Tibetan Plateau, rather than the elevated heating by the Tibetan Plateau (Boos and Kuang 2010; Boos and Kuang 2013). However, some other studies have proven that the thermal effects of the TP are the main driving force of the South Asian summer monsoon (Wu et al, 2012; Wu et al, 2015). Obviously, opinions differ in understanding the thermal forcing by the TP. One of the most important reasons is that high spatial and temporal resolution data on land-atmosphere interactions, which can be used in different climate models, are still lacking. To study the characteristics of land-atmosphere interactions in the TP, it is necessary to estimate the surface energy heat fluxes with fine spatial and temporal resolution over the TP.

Traditional surface energy flux measurements are not only expensive but also limited at the point scale. It is impossible to meet the need for a larger spatial scale with the complex terrain and landscapes of the TP. Remote sensing provides the possibility of deriving surface heat fluxes at a regional scale (Ma et al, 2002; Zhong et al, 2014). The methods of estimating surface energy flux by remote sensing can be roughly divided into two categories: the empirical (semiempirical) model and the theoretical model. The

Atmos. Chem. Phys. Discuss., https://doi.org/10.5194/acp-2018-1165
Manuscript under review for journal Atmos. Chem. Phys.
Discussion started: 20 December 2018

empirical (semiempirical) model is mainly based on an empirical formula between surface energy fluxes and surface characteristic parameters. The method itself is simple, but its applicability is limited. The basis of the theoretical model is the surface energy balance equation. The physical model mainly includes a single source model and a double source model. The single source model does not distinguish vegetation transpiration and soil evaporation but tends to consider them as a whole (Su，2002；Jia et al，2003；Roerink et al，2000; Bastiaanssen et al，1998；Allen et al，2007). The double source model separates the vegetation canopy from the soil and calculates the soil temperature and canopy temperature. Then, the sensible heat flux and latent heat flux are also calculated (Norman et al, 1995; Sánchez et al，2008).

Some studies have been carried out to estimate surface energy fluxes over the TP based on polar orbiting satellite data. Ma et al. (2003) estimated the surface energy flux of the CAMP (CEOP Asia–Australia monsoon project)/Tibet area using NOAA-14/AVHRR data. The results show that the estimated surface energy flux is in good agreement with the in situ measurements. Oku et al. (2007) used land surface temperature derived from Geostationary Meteorological Satellite (GMS)-5 and other essential parameters from NOAA-AVHRR, ERA-40 to estimate land surface heat fluxes for regions above 4000 m over the TP. However, the coarse resolution of EAR-40 (25 km) and large error of LST (more than 10 K) brought large uncertainties in final results. Ma et al. (2009) estimated the surface characteristic parameters and surface energy flux of the northern Tibetan Plateau in summer, winter and spring using a parameterized scheme for ASTER satellite data. Chen et al. (2013a) used observations from 4 sites in the TP to evaluate the results of the SEBS model and optimize the thermodynamic roughness parameterization scheme for underlying surface of bare soil. Based on Landsat TM/ETM+ data, Chen et al. (2013b) derived the surface energy flux of the Mount Everest area by using the enhanced SEBS model (TESEBS), which takes the influence of terrain factors on the solar radiation into account, and the SEBS model. The results show that the estimated results from the TESEBS model are superior to those from the SEBS model.

At present, the estimation of the surface energy flux of the TP is mainly based on polar orbit satellite data. Because of the low temporal resolution of the polar orbit satellites, time series of land-atmosphere energy and water exchange data with high temporal resolution in the TP have not been retrieved to date, and the effective basic parameters for the climate model cannot yet be provided. In addition, one of the basic characteristics of the atmospheric boundary layer is its diurnal variation, and information on daily variations in surface energy flux is also lacking over the TP. Furthermore, in previous studies of surface energy flux estimation, the accuracy of the model estimation is usually validated directly by the in situ measurements. The "energy closure" problem existing in the surface flux observation data has not received much attention, and the validation results have some uncertainties. Many previous studies have shown that there is a widespread "energy unclosed" problem in surface flux observations (Twine et al, 2000; Lee et al, 2002; Mauder et al, 2007; Yang et al, 2008). Pan et al. (2017) noted that the latent heat flux can be significantly underestimated by the eddy correlation method, while the Bowen ratio correlation method, which is based on the surface energy balance equation and the gradient diffusion theory of the surface layer, can effectively improve the underestimation of the latent heat flux.

This paper mainly focused on how to acquire time series of energy flux data with high temporal resolution using a combination of geostationary and polar orbiting satellite data. First, based on the surface flux measurements in the TP, the problem of "energy closure" in the observational data was improved by using the Bowen ratio calibration method. Then, the surface energy fluxes over the TP were estimated using the SEBS model with inputs from high temporal resolution land surface temperature from FY-2C data and other land surface characteristic parameters from polar orbiting satellite data. The derived land surface heat fluxes were validated by flux tower measurements and were also compared with GLDAS flux products. The study area and datasets used in this study are introduced in section 2. The model description is given in section 3, followed by the results and discussion in section 4. The main conclusions are drawn in section 5.

2. Study Area and Data

The TP, located in southwest China, has an area of approximately 2.5×10^6 km^2 (Fig. 1). It is the largest plateau in China. With an average elevation of approximately 4000 m, it is also the highest plateau in the world, and the high elevation can directly influence the middle and upper layers of the atmosphere. For a long time, due to the harsh climate conditions and complex topography of the TP, meteorological stations in this area have been not only sparse but also uneven. A total of 6 meteorological stations have been used to compare with model estimates. Although these 6 sites are not scattered throughout the entire TP, they include several major land cover types (Zhong et al, 2010), and their elevation varies from 3000 m to 5000 m (Table 1). These stations are the only stations currently available, and each station is equipped to make four-component radiation measurements, soil moisture and temperature measurements,

Atmos. Chem. Phys. Discuss., https://doi.org/10.5194/acp-2018-1165
Manuscript under review for journal Atmos. Chem. Phys.
Discussion started: 20 December 2018

Atmospheric Chemistry and Physics
Open Access
Discussions

eddy-covariance measurements and conventional observation items such as wind speed (u), air temperature (T_a), specific humidity (SH) and air pressure (P_s).

Both the geostationary satellite Feng Yun 2C (FY-2C) and the polar orbiting satellite SPOT are used to retrieve the essential land surface characteristic parameters. The stretched visible and infrared spin scan radiometer (SVISSR) onboard FY-2C is used to derive the hourly land surface temperature (LST) with a spatial resolution of 5 km following the algorithms developed by our group (Hu et al, 2018). We should point out here is that SVISSR has no infrared channel, which would be needed to derive NDVI, albedo and emissivity. Suppose that these parameters (NDVI, albedo and emissivity) have little variation during a day; then, the product of the orbiting satellite SPOT is used instead. The spatial resolution for NDVI, albedo and emissivity is 1 km with a daily temporal resolution.

A forcing dataset developed by the Institute of Tibetan Plateau Research, Chinese Academy of Sciences (ITPCAS), is used as model input in this study. The dataset has merged the observations from 740 operational stations of the CMA with the corresponding Princeton global meteorological forcing dataset (He, 2010; Yang et al, 2010). The parameters used in this study are downward shortwave radiation (R_{swd}), downward longwave radiation (R_{lwd}), wind speed, air temperature, specific humidity and air pressure. All these parameters have a spatial resolution of 10 km and a temporal resolution of 3 hours (Table 2).

Since 6 stations in Table 1 were not used in ITPCAS forcing data, they can be used as independent data to validate the accuracy of forcing meteorological data. The RMSE (root mean square error), MB (mean bias), MAE (mean absolute error) and R (correlation coefficient) are used to make a comparison between ITPCAS forcing data and in situ meteorological data.

$$RMSE = \sqrt{\frac{\sum_{i=1}^{N}(x_i - obs_i)^2}{N}} \tag{1}$$

$$MB = \frac{\sum_{i=1}^{N}(x_i - obs_i)}{N} \tag{2}$$

$$\mathrm{MAE} = \frac{\sum_{i=1}^{N}|x_i - obs_i|}{N} \tag{3}$$

$$R = \frac{\sum_{i=1}^{N}(x_i - \bar{x})(obs_i - \overline{obs})}{\sqrt{\sum_{i=1}^{N}(x_i - \bar{x})^2}\sqrt{\sum_{i=1}^{N}(obs_i - \overline{obs})^2}} \tag{4}$$

where x_i and obs_i are estimation and measurement, respectively. $\bar{x}$ and $\overline{obs}$ are the average values of estimation and measurement, respectively. As seen from Table 3, all six parameters show reasonable accuracy with in situ measurements, which means these forcing parameters can be used as model inputs.

Atmos. Chem. Phys. Discuss., https://doi.org/10.5194/acp-2018-1165
Manuscript under review for journal Atmos. Chem. Phys.
Discussion started: 20 December 2018

All of the above satellite data and forcing meteorological data have been processed with the spatiotemporal matching technique (Zou et al, 2018).

3. Model Description

Fig. 2 shows the general steps to derive the land surface heat fluxes in this paper. The SEBS model is used in this study. Because the surface energy balance has the four components of radiation (R_n), sensible heat flux (H_s), latent heat flux (LE) and soil heat flux (G_0), the energy balance equation can be written as

$$R_n = H_s + LE + G_0 \tag{5}$$

where R_n can be determined by the surface radiation equation as

$$R_n = R_{swd}(1-\alpha) + \varepsilon_a \sigma T_a^4 - \varepsilon_s \sigma T_s^4 \tag{6}$$

where R_{swd} is the downwelling solar radiation at the land surface. Because there are no infrared channels on board FY-2C, the NDVI, α and ε_s are derived from SPOT/VGT data. α is the broadband albedo, which can be derived from the narrowband reflectance of VGT $\alpha_1, \alpha_2, \alpha_3 and\ \alpha_4$ (Zou et al, 2018). $\alpha_1, \alpha_2, \alpha_3 and\ \alpha_4$ refer to reflectance of blue band, red band, near infrared band and short wave infrared band, respectively.

$$\alpha = -0.8141\alpha_1 + 0.4254\alpha_2 + 1.2605\alpha_3 - 0.2902\alpha_4 + 0.1819 \tag{7}$$

The σ in equation (6) is the Stefan-Boltzmann constant (5.76×10^{-8} W·m^{-2}·K^{-4}). ε_a and ε_s are the emissivities of surface air and the land surface, respectively. T_a and T_s are the surface air temperature and land surface temperature, respectively. The hourly T_s is derived from split window algorithms (Hu et al, 2018) based on two thermal bands of FY-2C.

The soil heat flux is determined by net radiation flux and vegetation coverage.

$$G_0 = R_n[\Gamma_c + (1-f_c)(\Gamma_s - \Gamma_c)] \tag{8}$$

where Γ_s and Γ_c are ratios of soil heat flux and net radiation flux for bare soil and full vegetation cover, respectively. f_c is vegetation coverage and can be derived from NDVI as follows.

$$f_c = \left(\frac{NDVI - NDVI_{min}}{NDVI_{max} - NDVI_{min}}\right)^2 \tag{9}$$

$$NDVI = \frac{\alpha_3 - \alpha_2}{\alpha_3 + \alpha_2} \tag{10}$$

By using the wind speed and air temperature at the reference height, the sensible heat flux, together with the friction velocity and Obukhov stability length, can be derived by solving the following nonlinear

Atmos. Chem. Phys. Discuss., https://doi.org/10.5194/acp-2018-1165
Manuscript under review for journal Atmos. Chem. Phys.
Discussion started: 20 December 2018

equations (11-13). Then, the latent heat flux can be estimated by applying equation (5).

$$L = -\frac{\rho \cdot c_p \cdot \theta_v \cdot u_*^3}{k \cdot g \cdot Hs} \tag{11}$$

$$u_* = k \cdot u \cdot \left[ln\left(\frac{z-d_0}{z_{0m}}\right) - \Psi_m\left(\frac{z-d_0}{L}\right) + \Psi_m\left(\frac{z_{0m}}{L}\right)\right]^{-1} \tag{12}$$

$$Hs = k \cdot u_* \cdot \rho \cdot c_p \cdot (\theta_0 - \theta_a) \cdot \left[ln\left(\frac{z-d_0}{z_{0h}}\right) - \Psi_h\left(\frac{z-d_0}{L}\right) + \Psi_h\left(\frac{z_{0h}}{L}\right)\right]^{-1} \tag{13}$$

where L is the Obukhov length, c_p is the specific heat at constant pressure, θ_v is the surface potential virtual air temperature, u_* is the friction velocity, $k = 0.4$ is the von Karman constant, g is the acceleration due to gravity, H_s is the sensible heat flux, u is the mean wind speed at reference height z, d_0 is the zero plane displacement height, z_{0m} is the roughness height for momentum transfer, z_{0h} is the roughness height for heat transfer, Ψ_m is the stability correction function for momentum heat transfer, Ψ_h is the stability correction function for sensible heat transfer and θ_0 and θ_a are the potential temperatures at the surface and reference height, respectively.

4. Results and Discussion

4.1 Validation Against In Situ Flux Tower Measurements

With the aid of SPOT/VGT and FY-2C/SVISSR data, the surface energy budget components have been estimated using the SEBS model. The accuracy of these estimates needs to be validated before further analyses. A total of 6 stations over the TP equipped with eddy-covariance measurements were selected for validation (Table 1). These validation stations cover a variety of climates, land cover types and elevations. The 'energy imbalance' is an important research issue and has been widely reported in former studies (Twine et al，2000；Wilson et al，2002；Wolf et al，2008；Majozi et al，2017；Pan et al，2017). If these measurements were not corrected and directly used to compare with estimates, some discrepancies would appear. Therefore, a so-called Bowen ratio correction method (Twine et al，2000；Wilson et al，2002; Hu et al, 2018) is used to process the in situ flux measurements. The results show that the energy closure ratio can be improved by approximately 20% for different stations (Hu et al, 2018). Then, the corrected in situ flux measurements are used to validate the satellite estimates. As shown in Fig. 3, the estimates of surface energy budget components show reasonable agreement with in situ measurements. The RMSEs for the net radiation flux, sensible heat flux, latent heat flux and soil heat flux are 76.63 Wm^{-2}, 60.29 Wm^{-2}, 64.65 Wm^{-2} and 37.5 Wm^{-2}, respectively. The total validation numbers (N) are more than 3837 to make the results much more representative and convincing. To test the robustness of our results, the surface energy budgets obtained from the Global Land Data Assimilation System (GLDAS) are selected for comparison with FY-2C estimations. The GLDAS products are produced by combining satellite and ground-based observations using advanced land surface modeling and data assimilation techniques (Zhong et al, 2011). These products have been proved to simulate key variables and fluxes with high accuracy (Rodell et al, 2004). Here, 3-hour land surface heat flux products with a spatial resolution of 25 km are selected for comparison with satellite estimates. The comparison shows that the accuracies of surface energy budgets from satellite estimation are much higher than those of GLDAS products (Table 4). The RMSE of the net radiation flux is reduced from 114.32 Wm^{-2} to 76.63 Wm^{-2}, while the values for sensible heat flux, latent heat flux and soil heat flux are reduced from 67.77 Wm^{-2}, 75.6 Wm^{-2} and 40.05 Wm^{-2} to 60.29 Wm^{-2}, 64.65 Wm^{-2} and 37.5 Wm^{-2}, respectively. Therefore, the new energy budget products not only have a finer spatial (10 km) and temporal resolution (hourly) than traditional polar orbiting satellite retrievals but also possess much higher accuracy than data assimilation results from GLDAS. Although SEBS algorithm was used in this study and Oku et al. (2007) (Oku 07 hereinafter), the methods to derive the land surface characteristic parameters, such as land surface temperature and albedo are different (Hu et al., 2018; Oku and Ishikawa 2004; Zou et al., 2018). The higher accuracy and finer spatiotemporal resolution of input forcing data (10km, 3 hour) and land surface characteristic parameters derived from satellites make our results superior than Oku 07. It should also be noted that there is only one station used to do the validation in Oku 07 while six stations with four major land cover types were used in this study to make the results much more robust. Moreover, our results cover the entire TP while Oku 07 only cover the region above 4000 m in the TP.

However, that there are indeed some discrepancies for this new product should be pointed out here, which means some room is still available to improve current products. The error sources may come from multiple aspects, such as the uncertainties of input forcing data, the accuracy of land surface parameters from satellite retrievals and some assumptions and simplification in the SEBS model itself. Furthermore, the mismatch between in situ measurements at the point level and the scales at the pixel level or grid level may also cause some errors. According to Zou et al. (2018), the input variables of land surface temperature, air temperature, wind speed and humidity have the largest influences on the accuracy of land surface heat fluxes. As revealed by Hu et al. (2018), the MB for LST is approximately -0.1 K. However, there are clearly underestimations of the surface air temperature and wind speed of approximately -0.045 K and -1.1 m s^{-1}, respectively. Under a combination of land-atmosphere temperature difference and wind speed, the sensible heat flux is underestimated. The underestimation of net radiation can be explained by the negative deviations (-4.73 $W \cdot m^{-2}$ and -8.49 $W \cdot m^{-2}$, respectively) of the downward shortwave flux and longwave radiation flux. A positive deviation in land surface temperature leads to greater upward longwave radiation flux, and a negative deviation in air temperature causes less downward longwave radiation. According to the surface radiation balance equation (Eq. 2), the net radiation flux is underestimated. The overestimation of latent heat flux may be caused by the negative deviation of specific humidity with approximately -0.76×10^{-4} $kg \cdot kg^{-1}$. This result occurs because less water vapor and higher land surface temperature promote more evapotranspiration.

4.2 Multitemporal and spatial distribution of surface energy budget components

One-year observation data and satellite estimations at BJ station were selected for comparison. As shown in Fig. 4, the satellite results can reproduce both the diurnal and seasonal surface flux variations very well. At the daily temporal scale, all the surface heat fluxes increase with sunrise and reach their maximum at mid-day before decreasing again with sunset. A unique characteristic of the atmospheric boundary layer is its well-known diurnal variations. The diurnal pattern of surface heat fluxes is in agreement with the diurnal evolution of the surface atmospheric boundary layer because the surface energy budgets provide a driving force for the surface atmospheric boundary layer. Fig. 4 also shows that the flux values are usually positive during the day while they become negative in the night. This feature means that the dynamic and thermal contrasts of land and atmosphere are totally different between day and night. The daytime surface heat fluxes are much larger than the values at night. At the seasonal scale, the net radiation flux usually increases from January to its maximum in July. Then, it decreases again from July to December. The variation trends for sensible heat flux and latent heat flux are quite opposite. Because the TP is greatly influenced by the Asian monsoon system and the vegetation intensity usually increases from May to September (Zhong et al, 2010), the sensible heat flux usually decreases while the latent heat flux usually increases from the premonsoon season to the monsoon season. However, from the monsoon season to the postmonsoon season, the sensible heat flux increases while the latent heat flux decreases.

A clear diurnal variation in hourly sensible heat flux and latent heat flux maps over the entire TP is shown in Fig. 5. Similar to the diurnal variations of net radiation flux, the amplitude of the sensible heat flux is relatively small before sunrise. Then, the sensible heat flux increases quickly until it reaches its

Atmos. Chem. Phys. Discuss., https://doi.org/10.5194/acp-2018-1165
Manuscript under review for journal Atmos. Chem. Phys.
Discussion started: 20 December 2018

maximum at approximately 14:00 (local standard time). After this time, it decreases gradually and tends to be smooth at night. The spatial distribution of sensible heat flux is somewhat complicated. In general, because of the sparse vegetation coverage and limited soil moisture in the western TP, the sensible heat flux is much lower than those in other parts of the TP. The latent heat flux tends to be zero before sunrise. With more solar energy after sunrise and much more evaporation from the soil and transpiration of vegetation, the latent heat flux rises gradually and reaches its maximum at 14:00. The spatial distribution of latent heat flux is in good agreement with land surface status. In the southeastern part of the TP, the climate conditions are warm and wet. Thus, the vegetation density is much higher than that in the northwestern part. From southeast to northwest, the vegetation changes from forest, meadow, grassland to sands and gravels, and the latent heat flux decreases accordingly.

5. Conclusions and remarks

A typical characteristic of the atmospheric boundary layer is diurnal variation. For a long time, little knowledge has been acquired to understand plateau-scale land-atmosphere interactions, especially their energy and water transfers, because of the limitation of point-scale observation and the low temporal resolution of polar orbiting satellites. In this study, polar orbiting satellite data were used to retrieve land surface characteristic parameters such as NDVI, vegetation coverage, albedo and emissivity. These parameters can be considered to have relatively very small diurnal variation but large seasonal variation. For other parameters with more typical diurnal variations, such as land surface temperature, the geostationary satellite FY-2C was used to retrieve plateau-scale land-surface temperatures. Other parameters with typical diurnal characteristics, such as downward longwave and shortwave radiation, air temperature, specific humidity, wind speed and air pressure, were derived from ITPCAS data. Based on the SEBS model and the above inputs, a time series of hourly land-atmosphere heat flux data over the TP was derived using a combination of geostationary and polar orbiting satellite data. The new dataset has a fine spatial resolution of 10 km. According to the validation with 6 field stations (more than 3800 samples), the high correlation coefficients and low RMSEs indicate that the estimated land surface heat fluxes are in good agreement with ground truth. Furthermore, the estimates were also compared with GLDAS flux data, which were thought to have high accuracy. The results showed that most derived variables were superior to GLDAS data. Based on this new dataset, the diurnal cycle of land surface heat fluxes was clearly identified. Moreover, the seasonal variations were found to be influenced by the Asian monsoon system. This new dataset can help to understand and quantify the diurnal variations in the land surface heating field, which are very important for atmospheric circulation and weather changes in the TP, especially in winter and spring when the main heating source is from the land surface. This dataset can also help to evaluate the results of numerical models. The uncertainties of input forcing data, the accuracy of land surface parameters from satellite retrievals, the mismatch between different scales and some assumptions and simplification in the SEBS model itself lead to some discrepancies between estimation and observation. For the next step, it is worthwhile to examine subpixel surface heat fluxes using techniques such as the temperature-sharpening method. Additionally, the FY-4 satellite with much high spatial, temporal and spectral resolution will provide the opportunity to monitor land-atmosphere interactions in much more detail.

Data availability. The ground-based measurements used in this study were obtained from the Third Pole Environment Database (http://www.tpedatabase.cn/portal/MetaDataInfo.jsp?MetaDataId=43). The SPOT data can be downloaded from https://www.vito-eodata.be/PDF/portal/Application.html. The FY-2C data can be downloaded from http://satellite.nsmc.org.cn/portalsite/Data/DataView.aspx. The forcing data set for this study can be obtained from http://dam.itpcas.ac.cn/chs/rs/?q=data.

Author contributions. LZ designed the study and performed the SEBS model with help from YM and ZH. XW, MC and NG collected the analyzed the in-situ flux data and forcing data. YH and LZ retrieved the land surface parameters form FY-2C and SPOT data. LZ wrote the manuscript with help from YM and YF. All commented on the paper.

Competing interests. The authors declare that they have no conflict of interest.

Acknowledgements. This research was jointly funded by Strategic Priority Research Program of Chinese Academy of Sciences (Grant No. XDA20060101), the National Natural Science Foundation of China (Grant No. 41522501, 41875031, 41275028, 41661144043), the Chinese Academy of Sciences (Grant No. QYZDJ-SSW-DQC019) and CLIMATE-TPE (ID 32070) in the framework of the ESA-MOST Dragon 4 Programme.

References

Allen, R. G., Tasumi, M., Morse, A., Trezza, R., Wright, J. L., Bastiaanssen, W., Kramber, W., Lorite, I., and Robison, C. W.: Satellite-based energy balance for mapping evapotranspiration with internalized calibration (METRIC) - Applications. J. Irrig. Drain. Eng., 133(4), 395-406, DOI: 10.1061/(ASCE)0733-9437(2007)133:4(395), 2007.

Bastiaanssen, W. G., Menenti, M., Feddes, R. A., and Holtslag, A. A. M.: A remote sensing surface energy balance algorithm for land (SEBAL). 1. Formulation. J. Hydrol., 212, 198-212, DOI: 10.1016/S0022-1694(98)00253-4, 1998.

Boos, W. R., and Kuang, Z. M.: Dominant control of the South Asian monsoon by orographic insulation versus plateau heating. Nature, 463, 218-223, DOI: 10.1038/nature08707, 2010.

Boos, W. R., and Kuang, Z. M.: Sensitivity of the south Asian monsoon to elevated and non-elevated heating. Sci. Rep., 3(1192), DOI: 10.1038/srep01192, 2013.

Chen, X., Su, Z., Ma, Y., Yang, K., Wen, J., and Zhang, Y.: An improvement of roughness height parameterization of the Surface Energy Balance System (SEBS) over the Tibetan Plateau. J. Appl. Meteorol. Clim., 52(3), 607-622, DOI: 10.1175/JAMC-D-12-056.1, 2013a.

Chen, X., Su, Z., Ma, Y., Yang, K., and Wang, B.: Estimation of surface energy fluxes under complex terrain of Mt. Qomolangma over the Tibetan Plateau. Hydrol. Earth Syst. Sc., 17(4), 1607-1618, DOI: 10.5194/hess-17-1607-2013, 2013b.

He, J.: Development of surface meteorological dataset of China with high temporal and spatial resolution, M.S. thesis, Inst. of Tibetan Plateau Res., Chin. Acad. of Sci., Beijing, China, 2010.

Hu, Y., Zhong, L., Ma, Y., Zou, M., Xu, K., Huang, Z., and Feng, L.: Estimation of the land surface temperature over the Tibetan Plateau by using Chinese FY-2C geostationary satellite data. Sensors, 18, 376, DOI: 10.3390/s18020376, 2018.

Jia, L., Su, Z., van den Hurk, B., Menenti, M., Moene, A., De, Bruin H. A. R., Yrisarry, J. J. B., Ibanez, M., and Cuesta, A.: Estimation of sensible heat flux using the Surface Energy Balance System (SEBS) and ATSR measurements. Phys. Chem. Earth, Parts A/B/C, 28(1-3), 75-88, DOI: 10.1016/S1474-7065(03)00009-3, 2003.

Lee, X., and Hu, X.: Forest-air fluxes of carbon, water and energy over non-flat terrain. Bound.-Lay. Meteorol., 103(2), 277-301, DOI: 10.1023/A:1014508928693, 2002

Liu, X., and Chen, B.: Climatic warming in the Tibetan Plateau during recent decades. Int. J. Climatol., 20(14), 1729-1742, 2000.

Ma, W., Ma, Y., Li, M., Hu, Z., Zhong, L., Su, Z., Ishikawa, H., and Wang, J.: Estimating surface fluxes over the north Tibetan Plateau area with ASTER imagery. Hydrol. Earth Syst. Sc., 13(1), 57-67, DOI: 10.5194/hess-13-57-2009, 2009.

Ma, Y., Ma, W., Zhong, L., Hu, Z., Li, M., Zhu, Z., Han, C., Wang, B., and Liu, X.: Monitoring and modeling the Tibetan Plateau's climate system and its impact on east Asia. Sci. Rep., 7, 44574 , DOI: 10.1038/srep44574, 2017.

Ma, Y., Menenti, M., Feddes, R. A., and Wang, J.: The analysis of the land surface heterogeneity and its impact on atmospheric variables and the aerodynamic and thermodynamic roughness lengths. J. Geophys. Res.-Atmos., 113, D08113, DOI: 10.1029/2007JD009124, 2008.

Ma, Y., Su, Z., Koike, T., Yao, T., Ishikawa, H., Ueno, K. I., and Menenti, M.: On measuring and remote sensing surface energy partitioning over the Tibetan Plateau—from GAME/Tibet to CAMP/Tibet. Phys. Chem. Earth, 28(1-3), 63-74, DOI: 10.1016/S1474-7065(03)00008-1, 2003.

Ma, Y., Su, Z., Li, Z., Koike, T., and Menenti, M.: Determination of regional net radiation and soil heat flux over a heterogeneous landscape of the Tibetan Plateau. Hydrol. Process., 16(15), 2963-2971, DOI: 10.1002/hyp.1079, 2002.

Ma, Y., Zhong, L., Su, Z., Ishikawa, H., Menenti, M., and Koike, T.: Determination of regional distributions and seasonal variations of land surface heat fluxes from Landsat-7 Ehanced Thematic Mapper data over the central Tibetan Plateau area. J. Geophys. Res.-Atmos., 111, D10305, DOI: 10.1029/2005JD006742, 2006.

Majozi, N. P., Mannaerts, C. M., Ramoelo, A., Mathieu, R. S., Nickless, A., and Verhoef, W.: Analysing surface energy balance closure and partitioning over a semi-arid savanna FLUXNET site in Skukuza, Kruger National Park, South Africa. Hydrol. Earth Syst. Sc., 21(7), 3401-3415, DOI: 10.5194/hess-21-3401-2017, 2017.

Mauder, M., Oncley, S. P., Vogt, R., Weidinger, T., Ribeiro, L., Bernhofer, C., Foken, T., Kohsiek, W., De, Bruin HAR., and Liu, H.: The energy balance experiment EBEX-2000. Part II: Intercomparison of eddy-covariance sensors and post-field data processing methods. Bound.-Lay. Meteorol., 123(1), 29-54, DOI: 10.1007/s10546-006-9139-4, 2007.

Norman, J., Kustas, W. P., and Humes, K. S.: Source approach for estimating soil and vegetation energy fluxes in observations of directional radiometric surface temperature. Agr. Forest Meteorol, 77(3-

4), 263-293, DOI: 10.1016/0168-1923(95)02265-Y, 1995.

Oku, Y., and Ishikawa, H.: Estimation of land surface temperature over the Tibetan Plateau using GMS data. J. Appl. Meteorol., 43, 548-561, 2004.

Oku, Y., Ishikawa, H., Haginoya, S., and Su, Z.: Estimation of land surface heat fluxes over the Tibetan Plateau using GMS data. J. Appl. Meteorol. Clim., 46, 183-195, 2007.

Pan, X., Liu, Y., Fan, X., and Gan, G.: Two energy balance closure approaches: applications and comparisons over an oasis-desert ecotone. J. Arid Land, 9(1), 51-64, DOI: 10.1007/s40333-016-0063-2, 2017.

Qiu, J.: Monsoon Melee. Science, 340(6139), 1400-1401, DOI: 10.1126/science.340.6139.1400, 2013.

Rodell, M., Houser, P. R., Jambor, U., Gottschalck, J., Mitchell, K., Meng, C. J., Arsenault, K., Cosgrove, B., Radakovich, J., Bosilovich, M., Entin, J. K., Walker, J. P., Lohmann, D., and Toll, D.: The Global Land Data Assimilation System. B. Am Meteorol. Soc., 85(3), 381-394, DOI: 10.1175/BAMS-85-3-381, 2004.

Roerink, G. J., Su, Z., and Menenti, M.: S-SEBI: A simple remote sensing algorithm to estimate the surface energy balance. Phys. Chem. Earth, Part B: Hydrology, Oceans and Atmosphere, 25(2), 147-157, DOI: 10.1016/S1464-1909(99)00128-8, 2000.

Sánchez, J. M., Scavone, G., Caselles, V., Valor, E., Copertino, V. A., and Telesca, V.: Monitoring daily evapotranspiration at a regional scale from Landsat-TM and ETM+ data: Application to the Basilicata region. J. Hydrol., 351(1-2), 58-70, DOI: 10.1016/j.jhydrol.2007.11.041, 2008.

Seneviratne, S. I., and Stöckli, R.: The role of land-atmosphere interactions for climate variability in Europe [C]. Climate Variability and Extremes During the Past 100 years, Switzerland, Springer, 179-193, 2008.

Su, Z.: The Surface Energy Balance System (SEBS) for estimation of turbulent heat fluxes. Hydrol. Earth Syst. Sc., 6(1), 85-100, DOI: 10.5194/hess-6-85-2002, 2002.

Twine, T. E., Kustas, W. P., Norman, J. M., Cook, D. R., Houser, P., Meyers, T. P., Prueger, J. H., Starks, P. J., and Wesely, M. L.: Correcting eddy-covariance flux underestimates over a grassland. Agr. Forest Meteorol., 103(3), 279-300, DOI: 10.1016/S0168-1923(00)00123-4, 2000.

Wilson, K., Goldstein, A., Falge, E., Aubinet, M., Baldocchi, D., Berbigier, P., Bernhofer, C., Ceulemans, R., Dolman, H., Field, C., Grelle, A., Ibrom, A., Law, B. E., Kowalski, A., Meyers, T., Moncrieff, J., Monson, R., Oechel, W., Tenhunen, J., Valentini, R., and Verma, S.: Energy balance closure at

FLUXNET sites. Agr. Forest Meteorol., 113(1), 223-243, DOI: 10.1016/S0168-1923(02)00109-0, 2002.

Wolf, A., Saliendra, N., Akshalov, K., Johnson, D. A., and Laca, E.: Effects of different eddy covariance correction schemes on energy balance closure and comparisons with the modified Bowen ratio system. Agr. Forest Meteorol., 148(6-7), 942-952, DOI: 10.1016/j.agrformet.2008.01.005, 2008.

Wu, G., Duan, A., Liu, Y., Mao, J., Ren, R., Bao, Q., He, B., Liu, B., and Hu, W: Tibetan Plateau climate dynamics: recent research progress and outlook. Natl. Sci. Rev., 2, 100-116, DOI: 10.1093/nsr/nwu045, 2015.

Wu, G., Liu, Y., He, B., Bao, Q., Duan, A., and Jin, F.: Thermal controls on the Asian summer monsoon. Sci. Rep., 2, 404, DOI: 10.1038/srep00404, 2012.

Yang, K., and Wang, J.: A temperature prediction-correction method for estimating surface soil heat flux from soil temperature and moisture data. Sci. China Ser. D: Earth Sciences, 51(5), 721-729, DOI: 10.1007/s11430-008-0036-1, 2008.

Yang, K., He, J., Tang, W., Qin, J., and Cheng, CCK.: On downward shortwave and longwave radiations over high altitude regions: Observation and modeling in the Tibetan Plateau. Agric. Forest. Meteorol, 150, 38-46, 2010.

Ye, D., and Gao, Y.: Meteorology of the Qinghai-Xizang (Tibet) Plateau. Science Press, 278 pp, 1979.

Zhong, L., Ma, Y., Fu, Y., Pan, X., Hu, W., Su, Z., Salama, M.S., and Feng, L.: Assessment of soil water deficit for the middle reaches of Yarlung-Zangbo River from optical and passive microwave images. Remote Sens. Environ., 142, 1-8, DOI: 10.1016/j.rse.2013.11.008, 2014.

Zhong, L., Ma, Y., Su, Z., and Salama, M.S.: Estimation of land surface temperature over the Tibetan Plateau using AVHRR and MODIS data. Adv. Atmos. Sci., 27(5): 1110-1118, DOI: 10.1007/s00376-009-9133-0, 2010.

Zhong, L., Su, Z., Ma, Y., Salama, M. S., and Sobrino, J. A.: Accelerated changes of environmental conditions on the Tibetan Plateau caused by climate change. J. Climate, 24(4): 6540-6550, DOI: 10.1175/JCLI-D-10-05000.1, 2011.

Zou, M., Zhong, L., Ma, Y., Hu, Y., and Feng, L.: Estimation of actual evapotranspiration in the Nagqu river basin of the Tibetan Plateau. Theor. Appl. Climatol., 132(3-4), 1039-1047, DOI: 10.1007/s00704-017-2154-1, 2017.

Zou, M., Zhong, L., Ma, Y., Hu, Y., Huang, Z., Xu, K., and Feng, L.: Comparison of two satellite-based evapotranspiration models of the Nagqu River Basin of the Tibetan Plateau. J. Geophys. Res.-Atmos., 123, 3961–3975, DOI: 10.1002/2017JD027965, 2018.

Table 1: Ground measurement sites.

Sites	Longitude (°E)	Latitude (°N)	Elevation (m)	Land cover
BJ	91.899	31.369	4509.0	Plateau meadow
D105	91.943	33.064	5039.0	Plateau grassland
MS3478	91.716	31.926	4620.0	Plateau meadow
Linzhi	94.738	29.765	3326.0	Slope grassland
Nam Co	90.989	30.775	4730.0	Plateau grassland
QOMS	86.946	28.358	4276.0	Gravels

Table 2: Summary of the input datasets used for calculating land surface heat fluxes.

Variables	Data Source	Resolution	
		Spatial	Temporal
T_s	FY-2C/SVISSR	5 km	hourly
NDVI	SPOT/VGT	1 km	daily
P_v	SPOT/VGT	1 km	daily
α	SPOT/VGT	1 km	daily
ε_s	SPOT/VGT	1 km	daily
R_{swd}	ITPCAS	10 km	3-hour
R_{lwd}	ITPCAS	10 km	3-hour
u	ITPCAS	10 km	3-hour
T_a	ITPCAS	10 km	3-hour
SH	ITPCAS	10 km	3-hour
P_s	ITPCAS	10 km	3-hour

Table 3: The validation of forcing data.

Variables	RMSE	MB	MAE	R	N
R_{swd} (W·m^{-2})	68.50	-4.73	37.38	0.974	1048
R_{lwd} (W·m^{-2})	20.98	-8.49	16.98	0.954	1048
u (m · s^{-1})	1.71	-1.01	1.28	0.793	1440
T_a (K)	2.08	-0.045	1.08	0.975	1440
SH (kg · kg^{-1})	0.56×10^{-3}	-0.76×10^{-4}	0.37×10^{-3}	0.981	1438
P_s (hPa)	8.51	-2.25	6.53	0.865	1440

Table 4: Comparison of derived flux data product and GLDAS against in situ measurements (Units: Wm^{-2}).

Model	Indicators	Rn	H	LE	G_0	SWU	LWU
SEBS	**RMSE**	76.63	60.29	64.65	37.5	49.81	52.99
	MB	-3.11	-22.13	6.03	7.81	11.74	-34.93
	MAE	50.47	45.67	44.39	28.43	26.88	39.31
	R	0.935	0.789	0.792	0.791	0.900	0.798
	N	4720	4554	3865	3837	4898	4721
GLDAS	**RMSE**	114.32	67.77	75.60	40.05	56.97	45.18
	MB	23.43	27.88	-10.35	-4.00	-15.42	-28.06
	MAE	81.90	47.48	44.89	30.52	31.35	31.61
	R	0.836	0.807	0.660	0.755	0.779	0.870
	N	1633	1580	1341	1329	1633	1633

Atmos. Chem. Phys. Discuss., https://doi.org/10.5194/acp-2018-1165
Manuscript under review for journal Atmos. Chem. Phys.
Discussion started: 20 December 2018

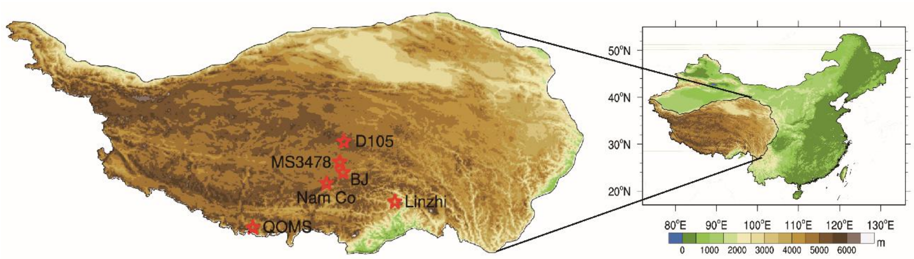

Figure 1: Location of the Tibetan Plateau. The pentagrams represent the eddy-covariance stations in the Tibetan Plateau.

Atmos. Chem. Phys. Discuss., https://doi.org/10.5194/acp-2018-1165
Manuscript under review for journal Atmos. Chem. Phys.
Discussion started: 20 December 2018

Atmospheric Chemistry and Physics
Open Access
EGU
Discussions

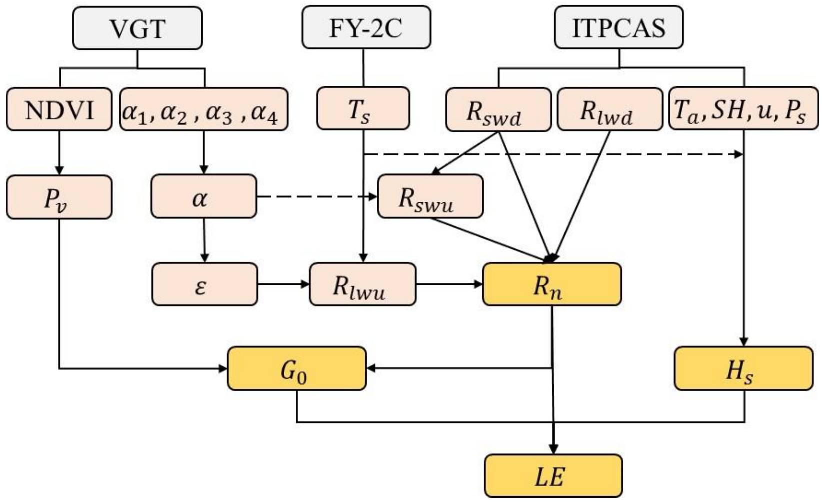

Figure 2: Flowchart of the flux estimation method.

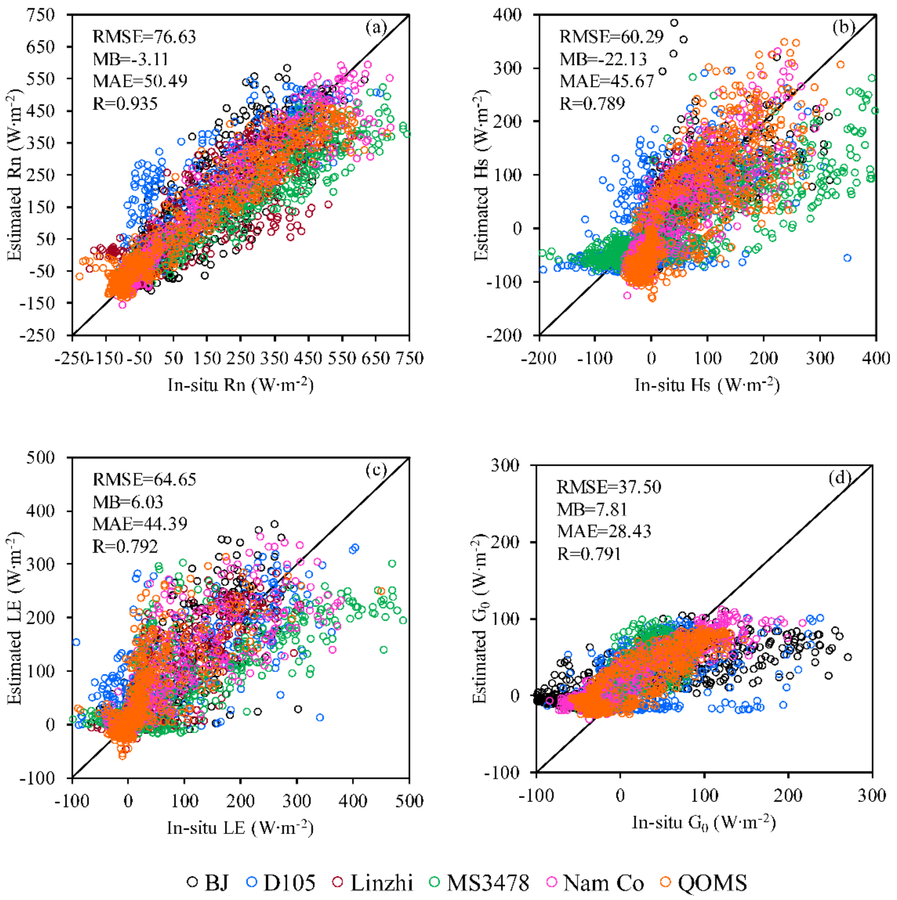

Figure 3: Validation of surface heat fluxes estimated by the SEBS model with in situ measurements (a. Net radiation flux; b. Sensible heat flux; c. Latent heat flux; d. Soil heat flux).

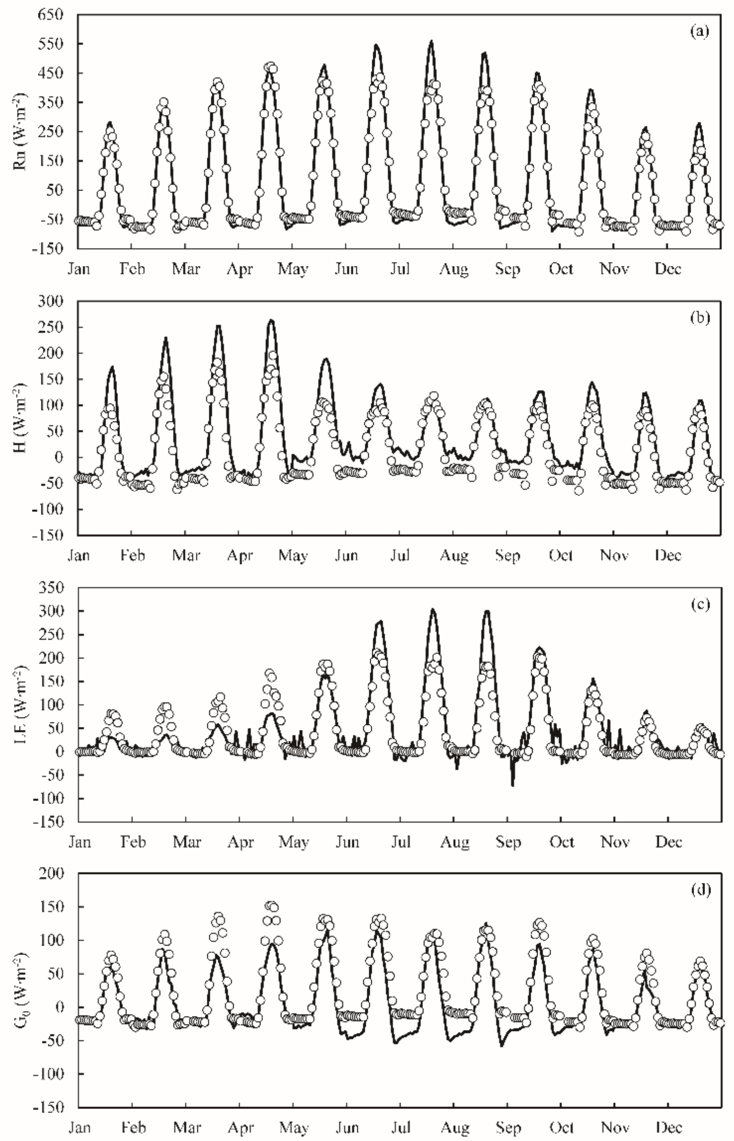

Figure 4: Time series of diurnal change in surface energy fluxes (units: Wm-2) observed by in situ measurements (curve) and those estimated by using the SEBS model (circle) at the BJ station in 2008.

5

Atmospheric Chemistry and Physics
Open Access
Discussions

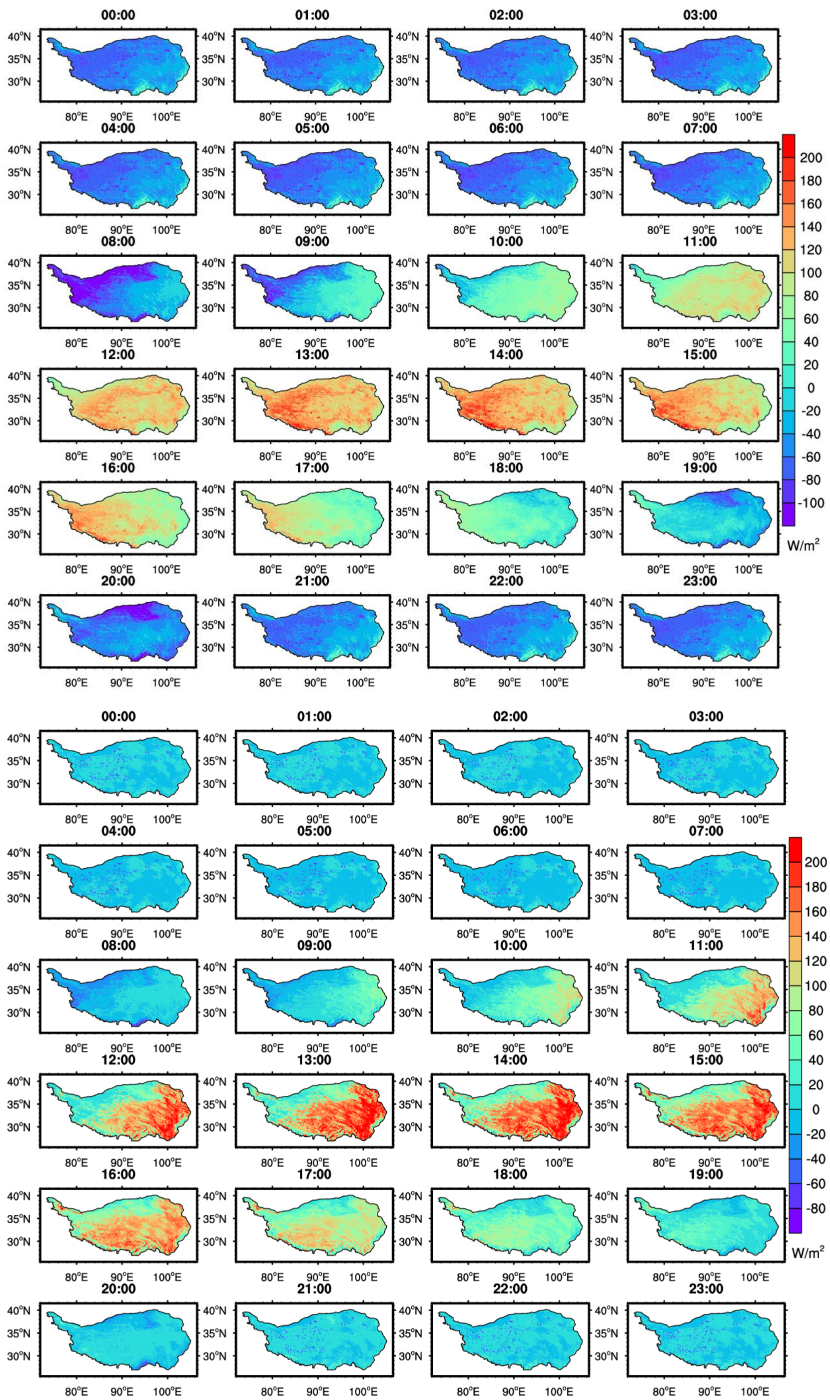

Figure 5: The spatial distribution and diurnal cycle of sensible heat flux (top panels) and latent heat flux (bottom panels) over the TP.